Experimental Heat Transfer, Fluid Mechanics, and Thermodynamics 2001
G. P. Celata, P. Di Marco, A. Goulas and A. Mariani

Active Control of Coaxial Jet Mixing and Combustion with Arrayed Micro Actuators

Naoki Kurimoto, Yuji Suzuki and Nobuhide Kasagi

Department of Mechanical Engineering, The University of Tokyo, Hongo Bunkyo-ku, Tokyo 113-8656, Japan
phone: +81 3 5841 6419, Fax: +81 3 5800 6999, E-mail: kurimoto@thtlab.t.u-tokyo.ac.jp

ABSTRACT

A novel coaxial jet nozzle equipped with a row of miniature electromagnetic flap actuators is developed for active control of flow mixing and combustion. The spatio-temporal flow structures of the coaxial jet were studied through flow visualization and quantitative measurements by using PLIF and LDV. The inner potential cone length becomes much shorter, and mixing between the inner and outer fluids is markedly enhanced by the flap motion. The most effective flapping frequency for mixing enhancement corresponds to Strouhal number of 0.9, which is close to the preferred mode frequency. A preliminary attempt at controlling the resultant combustion is also made of a methane-air lifted flame. The flame base is stabilized at the larger air-to-fuel velocity ratios by the flap motion at the optimum flapping frequency for mixing.

1. INTRODUCTION

Small-scale distributed generation (DG) systems are expected to play a major role to establish the energy security as well as to resolve the environmental issues in the East-Asian area. Unlike large-scale power plants, the energy released from fossil fuels can be utilized more systematically and efficiently so that the total consumption of resources and emission of carbon dioxide would be reduced. In order to make future DG systems really competitive in terms of energy saving and environment protection, we should drastically improve the energy conversion efficiency of central elements of DG systems, such as micro gas turbines and fuel cells, while reducing the toxic effluents.

It is a challenging technological target to reduce the emissions of toxic effluents such as NOx in small combustors with large load fluctuation such as those in micro gas turbines. In such a small capacity combustor, the mixing between fuel and air discharged is likely to be deteriorated, being associated with decrease in the Reynolds number. The mixing condition is considered to be deeply linked with prompt and thermal NOx formation because in general such process depends on local equivalent ratio and/or temperature distribution in a flame. Therefore, controlling mass, momentum and heat transport in turbulent combustion is considered to be a practically feasible way of suppressing NOx as well as unburned hydrocarbons. In addition, lean premixed combustion mode, which is often employed in gas turbines, can not always be maintained under the condition of large load fluctuation, because it is stable only in a relatively narrow fuel-to-air ratio range and easily blown off. Consequently, the combustion mode can often be changed into a diffusion combustion mode, with large emission of toxic effluents, even if it is designed to achieve a lean combustion mode in a rated operation.

Thus, in a combustion field with large load fluctuation, which often arises in micro gas turbines' combustors, it is difficult to always keep an ideal combustion mode using some passive devices such as a swirler and/or some flame holders, because they are designed to work effectively only under the designed condition. Therefore, a more advanced active control method is desired.

Combustion control has been studied by many researchers (e.g., MacManus *et al.*, [1]). Chao *et al.* [2] reported that the emissions of NOx and UHC can be reduced by making a flame lifted by acoustic excitations. They also reported that lifted flames can be stabilized by helical mode excitation using piezoelectric actuators [3].

Recently, active control of turbulent shear flows attracts much attention [4-6]. Since large-scale coherent structures emerging in various shear flows play a dominant role in the turbulent heat and momentum transport [7-9], selective manipulation of these structures is desired in order to obtain efficient control effect. Recent development of MEMS (Micro electro-mechanical Systems) technology enables us to fabricate micro actuators, which are small enough to impose direct control input on the coherent structures (Ho & Tai, [10]; McMichael, [11]). Liu *et al.* [12] showed that the rolling moment of a delta wing is efficiently controlled by micro magnetic flap actuators placed on the leading edge. Smith and Glezer [13] fabricated miniature zero-mass-flux jet actuators. They showed that a macro-scale planar jet can be vectored due to the formation of low-pressure recirculating flow regions near the flow boundary. Huang *et al.* [14] developed an on-chip electrostatic actuator integrated with a pressure sensor to detect and control screech in a high-speed air jet. Suzuki *et al.* [15] developed a novel axisymmetric nozzle, equipped with a row of miniature flap actuators on its nozzle lip, and investigated the response of the jet flow to various control modes. They found

that the entrainment rate of the jet is significantly increased when furcating jet is generated by adding disturbances locally into the jet shear layer.

The final goals of the present study are to achieve flexible control of shear layer mixing in order to manage distributions of local equivalent ratio and/or temperature, and consequently to achieve a stable combustion field with the low emissions of the toxic effluents. As the first step, Suzuki *et al.* [16] extended the control scheme developed by Suzuki *et al*. [15] to mixing enhancement of an isothermal water coaxial confined jet. They employed an coaxial nozzle having 18 miniature flap actuators on its outer annular lip in order to manipulate large-scale vortical structures emerging from the shear layer between the annular jet and the ambient still fluid. They found that the vortical structures are significantly strengthened with the artificial disturbances generated by the flaps, and thus the mixing between the inner and annular jets are markedly enhanced through the vigorous pinching of the central fluid.

In the present study, a similar control scheme is employed for an isothermal coaxial air jet, and the effect of flap motion on the mixing process is investigated through flow visualization and quantitative measurements with the aid of planar laser-induced fluorescence (PLIF). The flapping frequency is systematically changed in order to clarify the relationship between the optimum control mode and the preferred mode. Moreover, a preliminary attempt is made at controlling a flame by using these actuators.

2. EXPERIMENTAL SETUP

A coaxial nozzle equipped with miniature electromagnetic flap actuators is shown in Fig. 1. A coaxial air jet was issued vertically into an test section with 1000 mm height and 560 x 560 mm^2 square cross section. The central jet flow was supplied from a long straight tube with a diameter of D_i = 10 mm, in which a fully-developed laminar flow was established. The annular flow was discharged through a 42:1 area ratio nozzle with an exit diameter of D_o = 20 mm. By considering operation conditions of lean premixed combustions, measurements were made at a large velocity ratio r_u (= $U_{m,o}/U_{m,i}$) of 5.

Au & Ko [17] and Rehab *et al.* [18] separately showed that the outer jet dominates the near-field flow structure when the velocity ratio is large. Therefore, the electromagnetic flap actuators developed by Suzuki *et al.* [15] are placed inside the outer lip of the annular nozzle as shown in Fig. 1. The flap is made of a copper plated polyimide film having 9 mm in length and 3 mm in width. Film thickness is respectively 35 μm and 35 μm for the polyimide and copper layer. When an electric current is applied to the copper coil, the flap is elastically bent by the electromagnetic force between the coil and a cylindrical permanent magnet placed underneath. At the root of the flap, a part of the polyimide film is hollowed with a laser machining system to reduce the bending stiffness. In total, eighteen electromagnetic flap actuators were placed inside the nozzle exit at a regular interval and covered 86% of the circumference. Each flap is driven independently by a control signal from a multichannel digital-analog board. The maximum displacement of the flap was set to be about 1 mm. The flap actuator employed in the present study could not survive in high temperature circumstances such as in combustion chamber, but we concentrate on evaluating the active control scheme with an actuator currently available.

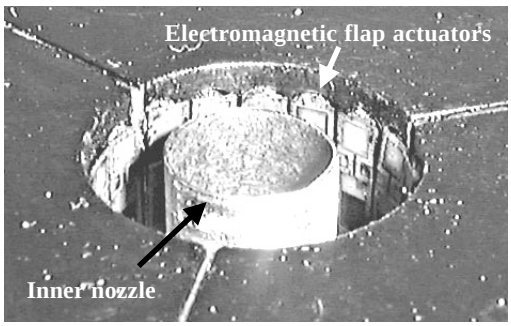

Figure 1. Coaxial jet nozzle equipped with electromagnetic flap actuators [15]

The bulk mean velocities of the central and annular parts of the nozzle are respectively set to be $U_{m,i}$ = 0.35 m/s and $U_{m,o}$ = 1.8 m/s (r_u = 5). The Reynolds number defined with the D_o and $U_{m,o}$ equals 2.2 x 10^3. The Cartesian coordinate system is employed, where x denotes the streamwise direction, while y and z are respectively the two perpendicular (vertical and horizontal) radial directions.

Concentration field of acetone was measured by using planar laser-induced fluorescence (PLIF) in order to access the effect of the present control scheme on the scalar mixing. The experimental setup is shown in Fig. 2. The inner jet air was saturated with acetone vapor by bubbling the air into a tank filled with the liquid. In order to keep the acetone vapor pressure at around 2.4 x 10^4 Pa, the temperature of the tank is kept at 18 ^{o}C by submerging the tank into a circulating water bath [19].

A frequency-doubled pulsed dye laser pumped by a tripled Nd:YAG laser (Lamda Physik SCANmate) was employed for excitation of the acetone vapor. Coumarin 153 dye was chosen to produce 270 nm UV light pulses of about 4 mJ/pulse. Linear-fluorescence regime could be ensured, because the laser power was considered to be too weak to cause absorption saturation [19]. The laser beam was introduced into the test section through a quartz window (120 x 120 mm^2) and formed into a laser sheet having about 0.3 mm in thickness through several cylindrical lens.

An image-intensified CCD camera (LaVision, Flamestar2; 576 x 384 pixels) was employed to capture the fluorescent images. The CCD chip of the camera was electrically cooled to -5^{o}C in order to reduce the noise by the dark current. The gain of the image intensifier was fixed at 8.0 counts/photon through out the present measurement. The whole system is synchronized by a trigger signal generated by a PC. The repetition rate of the image acquisition was about 2.5 flames/sec. The field of view was 60 x 40 mm^2 and the spatial resolution is 0.10 mm^2/pixel. The ICCD

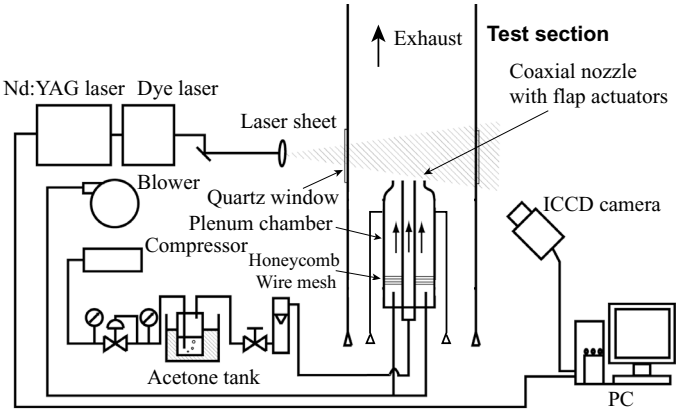

Figure 2. Schematic view of the experimental facility.

camera was equipped with a 100 mm UV lens as well as a low-pass optical filter (cutoff wavelength = 295 nm, LaVision) to eliminate the Mie scattering of the laser sheet from dust particles.

In addition to the PLIF measurement, velocity measurements were made by using a two-component fiber LDV (Dantec; 60X11) with a 4W Ar ion laser. At each measurement station, the statistics and the power spectra are computed from more than 15000 velocity samples at a sampling frequency on the order of 1000 Hz.

3. MIXING CONTROL

3.1. Flow Visualization and Velocity Measurement

Figure 3(a) shows a typical instantaneous image of a natural jet. The laser sheet cuts through the center of the jet axis. A laminar shear layer separates from the outer nozzle lip and roles up into vortex rings and these vortices pinch off the inner jet at $x/D_o \sim 2.5$. The mixing between the inner and outer fluids is small near the nozzle exit, and the intensity of the acetone fluorescence is almost constant along the jet axis up to $x/D_o \sim 1.5$. A similar phenomenon was observed in our previous study in a confined coaxial water jet [16].

Figures 3(b), (c) and (d) show typical instantaneous images of the jet controlled by axisymmetric flap motion (Axisymmetric Mode, hereafter), in which all eighteen flaps are driven in phase by a square-wave signal at f_a = 27 Hz, 80 Hz and 153 Hz. The Strouhal number based on f_a , D_o, and $U_{m,o}$ is 0.3, 0.9 and 1.7 respectively. It is observed that strong vortex rings are shed synchronized with the flap motion and the mixing is enhanced significantly, if compared to the natural jet. The length of the inner potential cone is dramatically shortened to about one half of that of the natural jet.

The preferred mode Strouhal number [20] measured at x/D_o = 3.0 at which the fundamental frequency is most amplified, is 0.7-0.9, while the column mode Strouhal number for the natural jet at x/D_o = 3.0 is 0.57. When the jet is controlled at St = 0.3, it is clearly observed that one large scale vortex ring strengthened by the flap motion is followed by two smaller scale vortex rings generated spontaneously by the shear layer instability as shown in Fig. 3(b), since the flapping frequency is almost one third of the preferred mode frequency. On the other hand, when St = 0.9, which is close to the preferred mode Strouhal number, vortex rings are shed synchronized with the flap motion. It is observed that a vortex ring produced periodically in the outer shear layer induces another vortex ring in the inner shear layer, and they evolve and grow downstream rapidly into much stronger vortex rings than those observed in the controlled jet at the other Strouhal numbers, pinching off the downstream end of the inner potential cone as shown in Fig. 3(c). Thus, the mixing between the inner and outer fluids is enhanced dramatically by transporting the inner fluid away from the jet axis. When St = 1.7, smaller and weaker vortex rings are generated by the flap motion and they undergo pairing near the nozzle exit since the flapping frequency is approximately twice the preferred mode. The boundary of the inner and outer fluids is smeared out by the action of these smaller vortices, but mixing is not enhanced as shown in Fig. 3(d). Therefore, the mixing between the inner and outer fluids is enhanced most effectively at St = 0.9.

Suzuki *et al.* [15] employed almost the same actuators for controlling an axisymmetric jet. They found that when each half cluster of flaps are driven out of phase (Alternate Mode, hereafter), the jet clearly bifurcates into two branches and the entrainment is significantly enhanced. Figure 3(e) shows a typical instantaneous image of the jet controlled by the Alternate Mode of f_a = 80 Hz. An asymmetic vortex, which is much larger than that of Axisymmetric Mode, is observed at $x/D_o \sim 0.7$. The length of the inner potential cone is a little bit more shortened than that of Axisymmetric Mode.

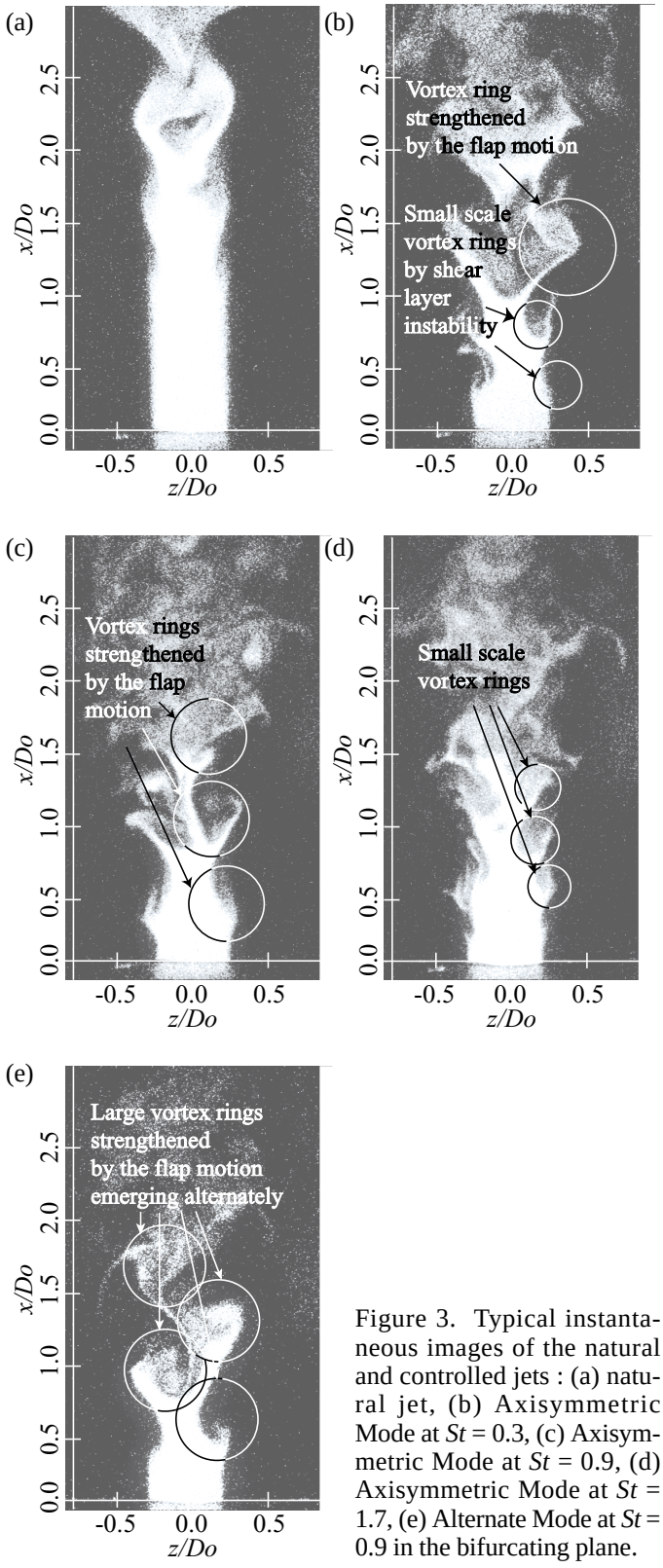

Figure 3. Typical instantaneous images of the natural and controlled jets : (a) natural jet, (b) Axisymmetric Mode at St = 0.3, (c) Axisymmetric Mode at St = 0.9, (d) Axisymmetric Mode at St = 1.7, (e) Alternate Mode at St = 0.9 in the bifurcating plane.

Figure 4 shows the profiles of the streamwise mean velocity U along the centerline. In the natural jet, U is slightly decreased near the nozzle exit and has the minimum value at x/D_o = 1.4, followed by a rapid increase due to the inrush of the outer vortex structures. On the other hand, for the controlled jets with Axi-

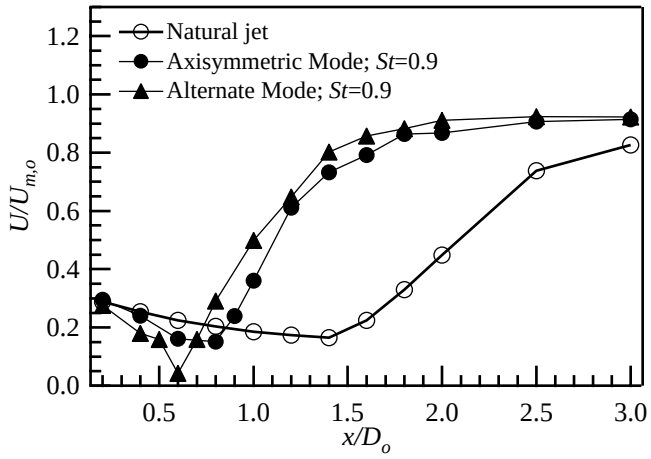

Figure 4. Streamwise mean velocity variations along the jet axis for the natural and controlled jet : Axisymmetric Mode at St = 0.9, and Alternate Mode at St = 0.9.

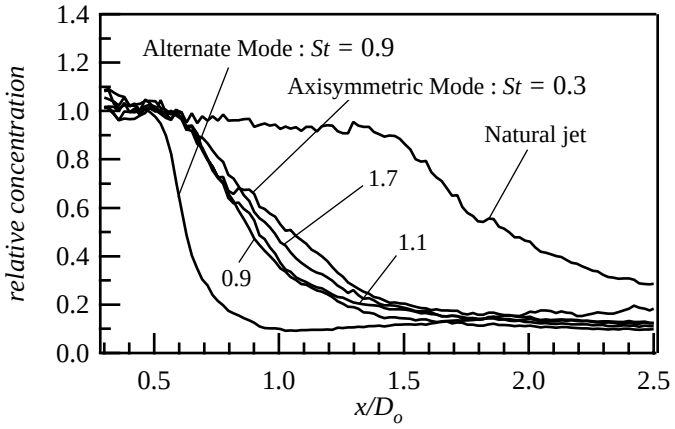

Figure 5. Mean concentration distributions of the natural and controlled jets.

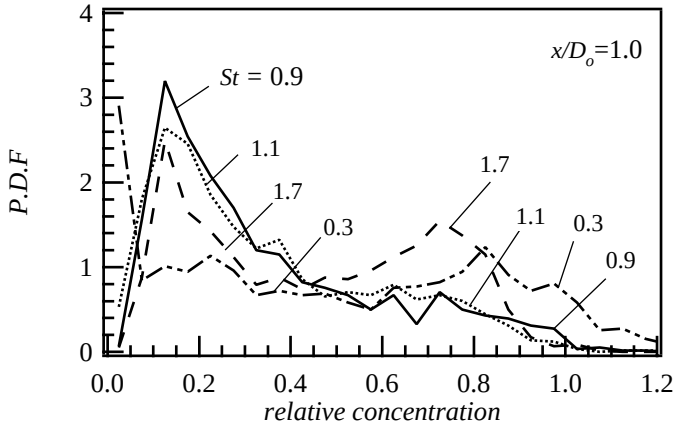

Figure 6. Probability density function of concentration of the controlled jets with Axisymmetric Mode at x/D_o = 1.0.

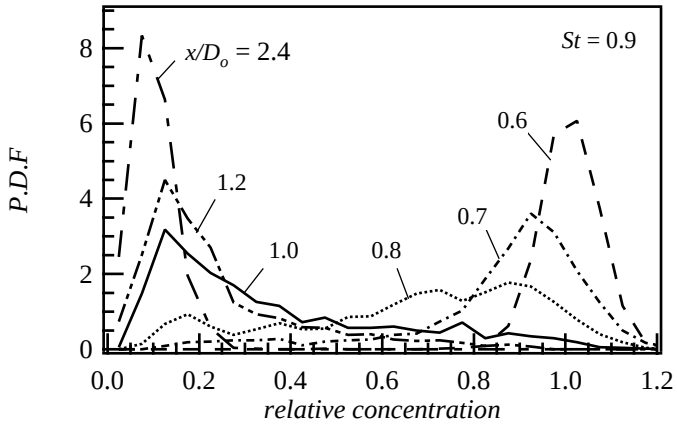

Figure 7. Probability density function of concentration of the controlled jets with Axisymmetric Mode at St = 0.9.

symmetric and Alternate Modes, U decreases within a short distance to the nozzle and rapidly increases. The minimum peak is shifted much closer to the nozzle exit. These results are in good accordance with the flow visualization results shown in Fig. 3.

The present data are also qualitatively in accordance with those of our previous measurement in a confined coaxial water jet [16]. However, the effect of the flap motion in the present experiment is somewhat smaller than that of Suzuki *et al*. [16], since the length of the inner potential cone in their controlled jet is about $0.5D_o$. Moreover, significant reverse flow at the end of the potential cone observed by Suzuki *et al*. [16] is almost absent in the present controlled jets. The reason of these discrepancies is not clear at this moment, but it is conjectured that the intensity of the disturbances generated by the flap motion relative to the jet exit velocity is smaller in the present air jet than in the previous water jet.

3.2. Concentration Distribution

Mean concentration of acetone is calculated with the fluorescence intensity obtained by PLIF. In total, 1164 instantaneous images are ensemble-averaged and the inhomogeneity of the laser intensity is compensated by using a reference image obtained for a quartz container filled with acetone vapor. The concentration is normalized by the fluorescence intensity at the potential cone end. Figure 5 shows fluorescence intensity distributions along the x axis for St = 0.3-1.9 at the z location where the inner potential cone takes the maximum value in its length. In the natural jet, the concentration of the inner fluid is kept at an almost constant value for $x/D_o < 1.5D_o$ and gradually decreased further downstream. In the jets controlled by Axisymmetric Mode, the length of the inner potential cone is shortened drastically and becomes about $0.6D_o$ for the Strouhal numbers examined. The jet controlled in Alternate Mode at St = 0.9 loses its concentration much more rapidly. These results are in good accordance with the velocity measurement results shown in Fig. 4. The potential cone length is relatively insensitive to the Strouhal number, but at St = 0.9, the mean concentration is rapidly decreased in the x direction.

Figure 6 shows the probability density function of concentration at x/D_o = 1.0 for various Strouhal numbers. At St = 0.3 and 1.7, the probability density remains to be relatively large in high concentration and there are two distinct peaks in concentration. Thus, although the mean concentration is significantly lower than that of the natural jet, the inner and outer fluids are only partially mixed at these Strouhal numbers. On the other hand, at St = 0.9, the probability density is completely shifted toward the lower concentration and the contribution in the low concentration range becomes maximum among various Strouhal numbers examined. Therefore, the mixing is enhanced most effectively at St = 0.9,

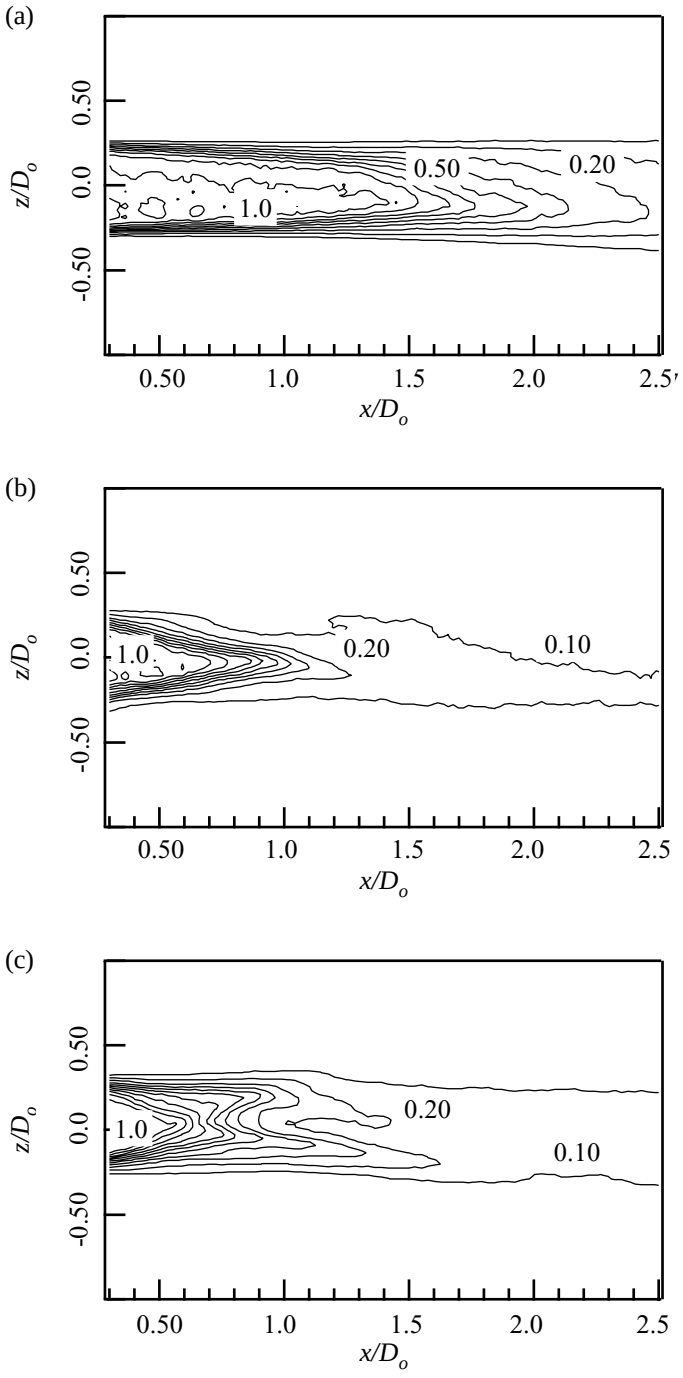

Figure 8. Contours of the mean concentration distribution of the natural and controlled jet : (a) natural jet, (b) Axisymmetric Mode at St = 0.9, (c) Alternate Mode at St = 0.45.

which is close to that of the preferred mode.

Figure 7 shows the probability density function at St = 0.9 for several x locations. Since there are only one peak in the probability density at any x location and the peak is smoothly shifted toward lower concentration with increasing x/D_o, the mixing between the inner and outer fluids should be actually enhanced.

Figures 8(a) and (b) show the contours of the mean concentration distributions of the natural and Axisymmetric controlled jets. It is evident that the mean concentration is deceased rapidly in all directions at St = 0.9. The contour of the mean concentration distribution in Alternate Mode at St = 0.45 is shown in Fig. 8(c). At St = 0.45, which is a subharmonic of the optimum flapping frequency for Axisymmetric Mode, the concentration distribution has two distinct peaks in the z direction at the

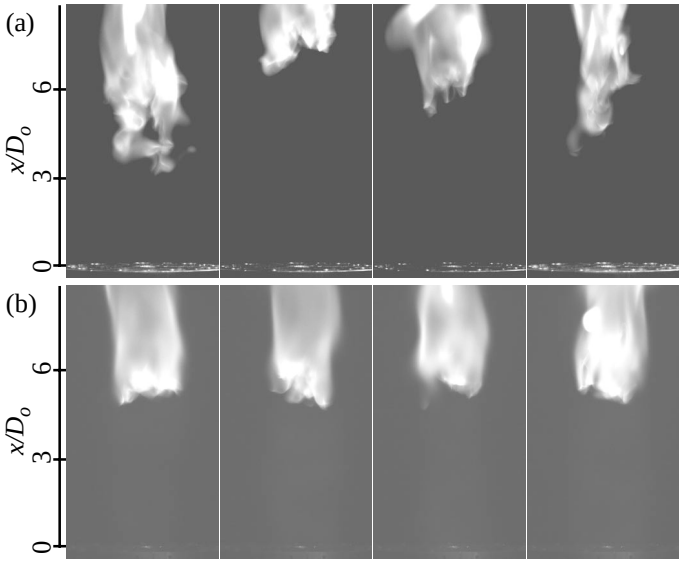

Figure 9. Instantaneous images of a lifted flame : (a) natural flame, (b) Axisymmetric controlled flame at St = 0.9.

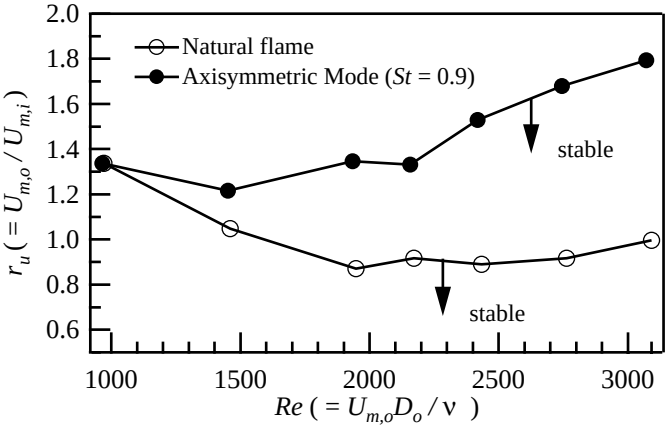

Figure 10. Stability limit of the natural and controlled flame with Axisymmetric Mode at St = 0.9.

downstream of $0.6D_o$. Then, it is considered that the coaxial jet controlled by Alternate Mode at St = 0.45 bifurcates and transports the inner fluid into two separate branches, and this fact is in accordance with the result of a single jet [15].

4. FLAME CONTROL

A preliminary attempt at controlling a resultant combustion field is carried out by using the same test section and coaxial nozzle equipped with the flap actuators. Methane is chosen as fuel, and introduced into the inner nozzle. A CCD camera (Lavision, FlowMaster; 1280 x 1024 pixels) is employed to capture flame images. The exposure time is set to be 10 msec.

Figures 9(a) and (b) show instantaneous images of the natural lifted flame ($U_{m,o}$ = 1.9 m/s , $U_{m,i}$ = 2.1 m/s, Re = 2.4 x 10^3) and the controlled lifted flame with Axisymmetric Mode at St = 0.9 ($U_{m,o}$ = 1.9 m/s , $U_{m,i}$ = 1.2 m/s, Re = 2.4 x 10^3). In the former case, the flame is held without any flame holder at this velocity ratio of 0.9. However, the flame is unstable and its base oscillates vigorously, and it is easily extinguished at larger velocity ratios. Since the location of the flame base roughly corresponds to the end of potential cone at this velocity ratio, it is conjectured that the oscillation of the flame base is due to periodic passage

of large-scale vortices.

On the other hand, when the flapping at Axisymmetric Mode at St = 0.9, which is the optimum flapping Strouhal number for mixing, is imposed, the lifted flame becomes more stable. This is probably because the large-scale vortices break into turbulence closer to the nozzle exit and their periodic passage at the flame base is suppressed, and also because well-mixed flammable gas is supplied to the flame base by the significant mixing enhancement of fuel and air in the controlled jet.

Figure 10 shows the maximum air-to-fuel velocity ratio, where the lifted flame is held at least for 3 minutes. It is found that for Axisymmetric Mode at St = 0.9, the flammable limit is extended to larger velocity ratios.

5. CONCLUSIONS

Active control with a raw of miniature flap actuators is applied to mixing enhancement and combustion control in a coaxial air jet. Flow visualization and quantitative measurement with LDV and LIF are made in order to evaluate the effect of the flap motion. The following conclusions can be derived:

1) The mixing between the inner and outer jets are markedly increased through the pinching-off mechanism by the strengthened vortex rings.
2) The optimum flapping Strouhal number for the mixing of the inner and outer fluids is 0.9, which is close to the preferred mode frequency.
3) The lifted flame under control becomes more stable and can be held at larger velocity ratios.

ACKNOWLEDGEMENTS

This work was supported through the research project on “Micro Gas Turbine/Fuel Cell Hybrid-Type Distributed Energy System” by the Department of Core Research for Evolutional Science and Technology (CREST) of the Japan Science and Technology Corporation (JST).

NOMENCLATURE

D_o - outer nozzle diameter of the coaxial nozzle, mm
D_i - inner nozzle diameter of the coaxial nozzle, mm
f_a - flapping frequency, Hz
r_u - velocity ratio of the outer jet to the inner jet velocity, dimensionless
Re - Reynolds number based on D_o and $U_{m,o}$, dimensionless
St - Strouhal number ($=f_aD_o/U_{m,o}$), dimensionless
$U_{m,o}$ - bulk mean velocity of the outer jet, m/s
$U_{m,i}$ - bulk mean velocity of the inner jet, m/s
x - streamwise distance from the exit of the coaxial nozzle, m

REFERENCES

1. McManus, K.R., Poinsot, T. and Candel, S.N., A Review of Active Control of Combustion Instabilities, Prog. in Energy Combust. Sci., 19, pp. 1-29, 1993.
2. Y.-C. Chao, T. Yuan and C.-S. Tseng, Effects of Flame Lifting and Acoustic Excitation on the Reduction of NOx Emissions, Combust. Sci. Tech., 113-114, pp. 49-65, 1996.
3. Y.-C. Chao, Y.-C. Jong and H.-W. Sheu, Helical-mode Excitation of lifted flames using piezoelectric actuators, Exp. in Fluids, 28, pp. 11-20, 2000.
4. Mankbadi, R., Dynamics and Control of Coherent Structure in Turbulent Jets, Appl. Mech. Rev., 45, pp. 219-248, 1992.
5. Moin, P., and Bewley, T., Feedback Control of Turbulence, Appl. Mech. Rev., 47, S3-S13, 1994.
6. Kasagi, N., Progress in Direct Numerical Simulation of Turbulent Transport and Its Control, Int. J. Heat & Fluid Flow, 19, pp. 128-134, 1998.
7. Crow S. C., and Champagne, F. H., Orderly Structure in Jet Turbulence, J. Fluid Mech., 48, pp. 547-591, 1971.
8. Cantwell, B. J., Organized Motion in Turbulent Flow, Annu. Rev. Fluid Mech., 13, pp. 437-515, 1981.
9. Robinson, S. K., Coherent Motions in the Turbulent Boundary Layer, Annu. Rev. Fluid Mech., 23, pp. 601-639, 1991.
10. Ho, C. M., and Tai, Y. C., Review: MEMS and Its Applications for Flow Control, ASME J. Fluids Eng., 118, pp. 437-447, 1996.
11. McMichael, J. M., Progress and Prospects for Active Flow Control Using Microfabricated Electromechanical Systems (MEMS), AIAA Paper, 96-0306, 1996.
12. Liu, C., Tsao, T., and Tai, Y. C., Out-of-plane Permalloy Magnetic Actuators for Delta-wing Control, Proc. 8th IEEE MEMS Workshop, Amsterdam, pp. 7-12, 1995.
13. Smith, B. L., and Glezer, A., Vectoring and Small Scale Motions Effected in Free Shear Flows Using Synthetic Jet Actuators, AIAA-paper, 97-0213, 1997.
14. Huang, C., Najafi, K., Alnajjar, E., Christophorou, C., Naguib, A., and Nagib, H. M., Operation Testing of Electrostatic Microactuators and Micromachined Sound Detectors for Active Control of High Speed Flows, Proc. 11th IEEE MEMS Workshop, Heidelburg, pp. 71-86, 1998.
15. Suzuki, H., Kasagi, N., and Suzuki, Y., Active Control of an Axisymmetric Jet with an Intelligent Nozzle, 1st Int. Symp. Turbulence & Shear Flow Phenomena, Santa Barbara, pp. 665-670, 1999; also submitted to Phys. Fluids.
16. Suzuki, Y., Kasagi, N., Horiuchi, Y., and Nagoya, D., Synthesized Mixing Progress in and Active-controlled Confined Coaxial Jet, 4th JSME-KSME Eng. Conf., Kobe, 3, pp. 469-474, 2000.
17. Au, H., and Ko, N. W. M., Coaxial Jets of Different Mean Velocity Ratios, J. Sound and Vib., 116, pp. 427-443, 1987.
18. Rehab, H., Villermaux, E., and Hopfinger, E. J., Flow Regimes of Large-velocity-ratio Coaxial Jets, J. Fluid Mech., 345, pp. 357-381, 1997.
19. Lozano, A., Yip, B., and Hanson, R. K., Acetone: a Tracer For Concentration Measurements in Gaseous Flows by Planar Laser-induced Fluorescence, Exp. Fluids, 13, pp. 369-376, 1992.
20. Zaman, K. B. M. Q., and Hussain, A. K. M. F., Vortex Pairing in a Circular Jet Under Controlled Excitation; Part 1. General jet response, J. Fluid Mech., 101, pp. 449-491, 1980.